

# EFFECT OF ANODIC OXIDATION ON THE CORROSION BEHAVIOR OF NICKEL-TITANIUM SHAPE MEMORY ALLOYS IN SIMULATED BODY FLUIDS (SBF)

S. Noori\* and J. Khalil-Allafi

\* s\_noori@sut.ac.ir

Received: November 2014

Accepted: March 2015

Research Center for Advanced Materials and Mineral Processing, Faculty of Materials Engineering, Sahand University of Technology, Tabriz, Iran.

**Abstract:** The effect of anodic oxidation of a NiTi shape memory alloy in sulfuric acid electrolyte on its surface characteristics was studied. Surface roughness was measured by roughness tester. Surface morphology was studied using optical microscopy (OM) and scanning electron microscopy (SEM). Corrosion behavior was specified by recording Potentiodynamic polarization curves and measuring the content of Ni ions, released into a SBF solution using atomic absorption spectroscopy (AAS). Fourier transformation infrared radiation (FT-IR) and energy dispersive spectroscopy were employed to verify the biocompatibility of the anodized and bare alloys after submersion in SBF. It was shown that anodic oxidation in sulfuric acid significantly increases corrosion resistance and biocompatibility. This layer improves corrosion resistance and Ni ion-release resistance by impeding the direct contact of the alloy with the corrosion mediums i.e. Ringer and SBF solutions. The TiO<sub>2</sub> oxide layer also decreases the releasing of Ni ions in to SBF solution.

**Keywords:** NiTi; oxidation; corrosion resistance; biocompatibility; Ni release.

## 1. INTRODUCTION

NiTi shape memory alloys are the materials, which have the ability to recover their prime shape with temperature and stress variations. They also have high corrosion resistance and good biocompatibility [1]. Therefore they have been employed in medical applications such as stents, surgery devices, orthodontic wires and implants [2-6].

Surface characteristics of NiTi shape memory alloys like corrosion resistance, Ni ion-release resistance and biocompatibility could be improved with the formation of a protective surface layer on the base metal [6-8]. There are many distinct methods to create the layer which are incomparable in many aspects and offer varying characteristics to the alloy. Among them it can be referred to methods such as diamond like carbon (DLC), plasma, gaseous and powder nitriding, electrochemical deposition, micro-arc oxidation, laser alloying, plasma spray, selective oxidation and surface melting [7, 9-18]. These methods are often complicated and they need multitude equipments. Therefore a simple and effective technique like anodic oxidation would

be so attractive. This method has been performed in various electrolytes such as sulfuric acid, acetic acid, phosphoric acid and etc. Shi and Cheng [19] attempted the anodization of NiTi in sulfuric acid and reported that the corrosion resistance of anodized NiTi was approximately 9 times better than that of bare NiTi. They also performed this procedure in methanol and obtained a thick layer which had a thickness of more than 10  $\mu\text{m}$  and was free of cracks [20]. Yang and Chen [21] studied the anodization of NiTi wires in sodium sulfate and created a Ni-free TiO<sub>2</sub> layer. Shi and Cheng [22] described the microstructure of oxide film formed on NiTi by anodization in acetic acid. They obtained an amorphous oxide film with yellowish interface color. The Ni/Ti atomic ratio at the surface of the anodized sample was approximately 10 times less than that obtained for bare NiTi. Chu and his coworkers [23] accomplished the anodization of NiTi in sulfuric acid. They reported the formation of a TiO<sub>2</sub> film with very low content of Ni which hinders emitting of Ni from NiTi SMA into SBF solution. Huang et al. [24] successively enhanced surface roughness and corrosion resistance of NiTi alloy by anodization in diluted HF solution.



Bayat et al. [25] studied the corrosion resistance of NiTi sputtered thin films by anodization. They found out that by varying the anodizing parameters such as voltage, the corrosion behavior of the anodized alloy can be changed.

In this study, the anodic oxidation of NiTi discs in sulfuric acid was studied. The main aim of this assay was the improvement of corrosion resistance, Ni ion-release resistance and biocompatibility which was done by development of a  $\text{TiO}_2$ -oxide layer on the surface of alloy.

## 2. EXPERIMENTAL

### 2.1. Sample Preparation

Disc samples with a diameter of 12.6 mm and a thickness of 1 mm were wire cut from a NiTi rod. The nominal composition of the alloy was Ti-50.8 at. % Ni. The samples were polished with SiC sandpapers down to 5000 grit and mechanically polished by 3 and 0.3  $\mu\text{m}$  alumina powders to achieve a mirror finish. Then they were cleaned in ultrasonic baths with acetone, ethanol and deionized water sequentially before leaving to dry in air at room temperature.

### 2.2. Anodizing Treatment

DC anodization was performed in a cell composed of NiTi as the anode, a graphite rod as the cathode and 3M sulfuric acid as the electrolyte. During the anodizing process, the electrolyte was stirred continuously by a magnetic bar with a speed of 120 rpm. The discs were anodized for 1 hour. The applied voltage was retained constant at 5 V. The samples were removed from the anodizing cell and dried in air after cleaning ultrasonically with acetone, ethanol and de-ionized water. After completion of the anodizing process for each specimen, the electrolyte solution was refreshed for subsequent sample. The mentioned anodizing parameters were selected after a procedure involving varying different anodizing parameters until reaching an even oxide layer which lays through the whole alloy surface. Anodizing voltage and stirring speed of electrolyte were set to be less or more

than the mentioned values, the obtained oxide layer was not even. For high values, outer parts of the circular surface were deprived of the existence of a protective layer and for low values it was true for the central part. It can be related to the threshold value of current density that is required for the formation of an oxide layer. For low values, only the current density of the outer parts reaches to this threshold. Therefore the oxide layer does not form in central parts of the surface. For high values, the current density of outer parts exceeds this threshold and results in dissolution of oxide layers in these areas.

### 2.3. Sample Characterization

The surface morphologies of bare alloy (in both as-polished and etched state) and anodized sample were studied using optical microscopy (OM, Olympus PMG3). The etchant solution was 100ml Hydrochloric acid, 20 ml de-ionized water, 2.4g Ammonium hydrogen difluoride, 34.5g Potassium metabisulfite. Complementary surface morphology studies were performed using scanning electron microscopy (SEM, Cam Scan MV2300) and field emission scanning electron microscopy (FESEM, Hitachi S4160). SEM was used for bare sample and FESEM was used for anodized sample which needed more resolution. The study of the cross-section morphology and the measurement of roughness of the anodized samples were carried out using FESEM and surface roughness tester (Surtronic 25) respectively. The roughness test was carried out in conformity with standard ISO 4288-1996.

The Potentiodynamic polarization tests were performed in SBF and Ringer solutions at 37°C and pH=7.4 [26-27]. The compositions of the solutions are listed in tables 1 and 2. Platinum sheet worked as counter electrode and the potential was expressed in regard to a saturated calomel electrode (SCE). The anodic polarization curves were recorded with a scanning rate of 1 mV/s. The test was carried out in accordance with ASTM standard G 61-68. Figure 1 is the samples were put in a holder, described in ASTM standard G 61-68, and were retained in the corrosion mediums i.e. SBF and Ringer solutions, until the corrosion tests were accomplished. 1  $\text{cm}^2$  of the

**Table 1.** Chemical composition of SBF solution [19].

Component	Concentration
NaCl	8.036 g
NaHCO <sub>3</sub>	0.352 g
KCl	0.225 g
K <sub>2</sub> HPO <sub>4</sub> .3H <sub>2</sub> O	0.230 g
MgCl <sub>2</sub> .6H <sub>2</sub> O	0.311 g
HCl 1M	40 ml
CaCl <sub>2</sub>	0.293 g
Na <sub>2</sub> SO <sub>4</sub>	0.072 g
Tris	6.063 g
HCl 1M	0 - 0.2 ml

**Table 2.** Chemical composition of Ringer solution [20].

Component	Concentration
NaCl	0.86 g
KCl	0.03 g
CaCl <sub>2</sub> . 2H <sub>2</sub> O	0.033 g

were immersed in SBF solution for 1, 3, 5, 15 and 31 days and Ni content was investigated by atomic absorption spectroscopy (AAS, Nova 2300).

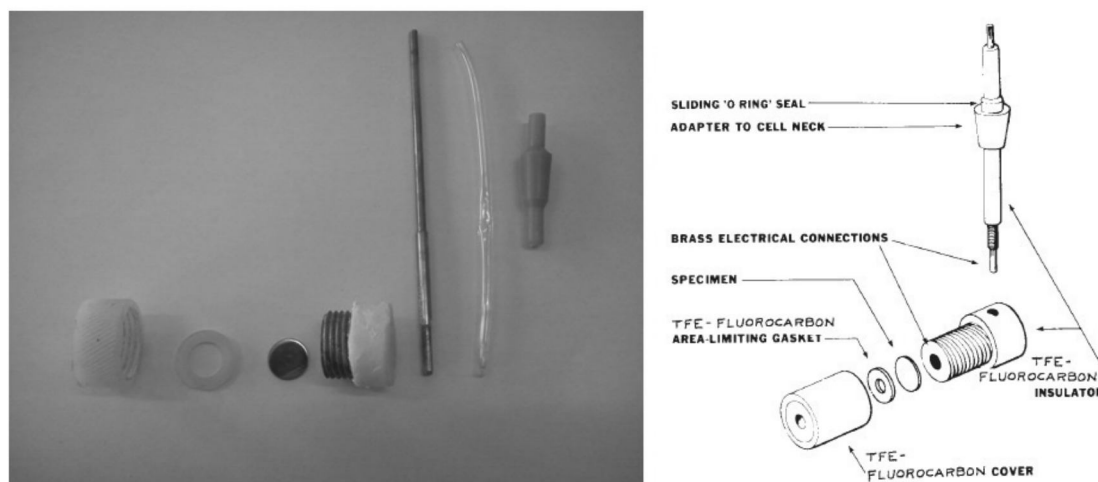
To evaluate the formation of apatite on the surface of NiTi anodized samples in comparison with bare NiTi, the samples were submersed in the SBF with  $T=37^{\circ}\text{C}$  and  $\text{pH}=7.4$ . The ratio of solution volume to surface area of the samples was about  $0.4 \text{ ml/mm}^2$ . The samples were analyzed using energy dispersive spectroscopy (EDS) and Fourier transform infrared spectroscopy (FT-IR, Unicam 4600) after removal out of the SBF.

surface area of the samples was exposed to corrosion medium. The parameters of  $i_{\text{corr}}$  and  $R_p$  (polarization resistance which is inversely related to corrosion current density) were extracted from polarization curves. They were calculated by linear polarization method using ASTM G-59.

For Ni-release experiments, NiTi samples

### 3. RESULTS AND DISCUSSION

A few studies have presented optical micrographs of the surfaces of the anodized and bare samples. However here, in figure 2, optical micrographs of the surfaces of as-polished, etched and anodized samples have been

**Fig. 1.** Holder of samples that described in ASTM standard G 61-68.



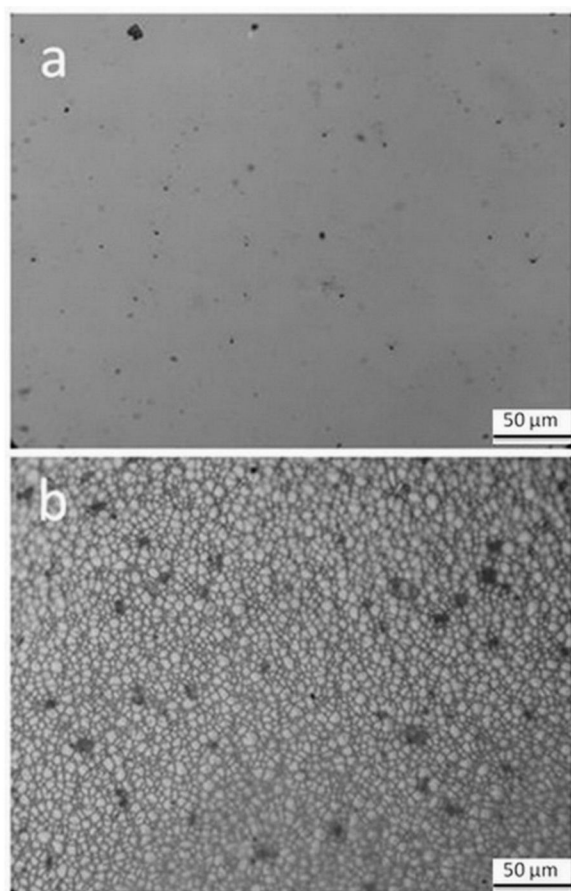


**Fig. 2.** Optical micrographs of the surfaces of the (a) bare and (b) anodized samples.

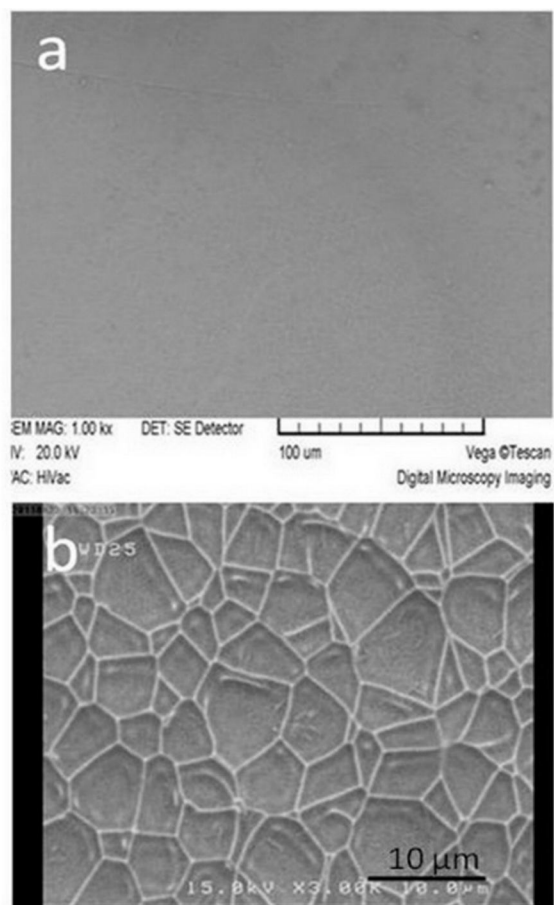


**Fig. 3.** FESEM micrographs of the surfaces of the (a) bare and (b) anodized samples.

displayed. OM image of the etched sample has been displayed because it is possible for the viewer to mistake the boundaries observed on the surface of anodized samples for the grain boundaries of the bare sample. It is clearly seen that the boundaries that are observed on anodized and etched specimens are completely different. Also comparison of figures 1-a and 1-c shows a drastic change in NiTi surface morphology due to anodization process. As can be seen, the as-polished surface of bare NiTi is smooth while after anodizing, protrusive lines are appeared on the surface which results in the creation of a rough surface. The mentioned boundaries are also clearly seen in FESEM image of the surface of anodized sample (Figure 3). The boundaries have produced protrusions on the surface. These protrusions can create a mechanical contact between the implant and the body environment.

This is the answer of this question that why the amount of hydroxyl apatite deposition on the surface of anodized alloys is much higher than that on the surface of bare alloys.

The results of roughness measurements also confirm above microscopy observations. The mean roughness  $R_a$  of the anodized sample has been measured about 480 nm which is much larger than that came by bare sample (33 nm). This roughness is partially related to more positive formation energy of nickel oxide relative to titanium oxide which results in participation of titanium in anodization rather than nickel [28].

Figure 4 is the cross-sectional FESEM images of the anodized NiTi sample. The thick oxide layer, formed due to anodization is clearly visible. This layer has a thickness of about 13  $\mu\text{m}$ . It is well known that the thickness of the layer intensively depends on the anodizing parameters

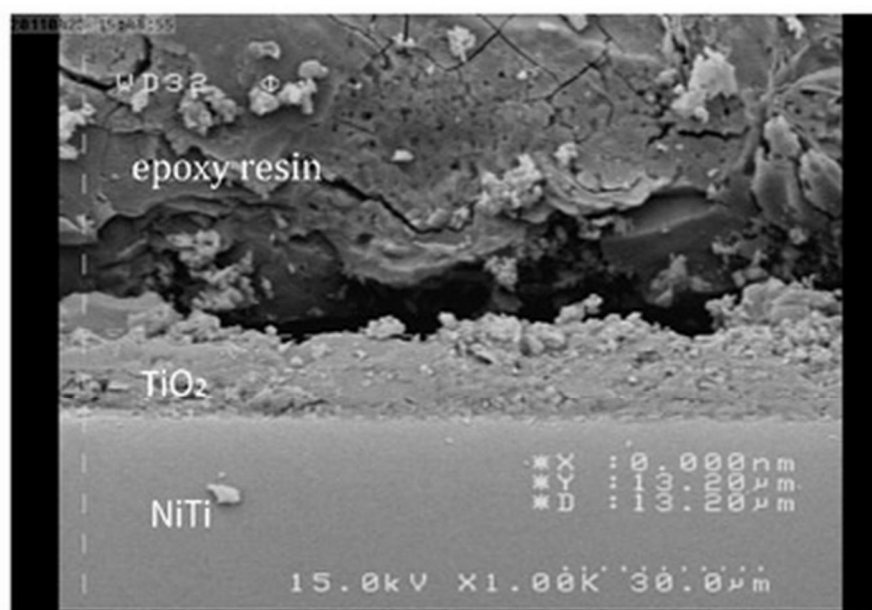


Fig. 4. Cross-sectional FESEM image of the anodized sample.

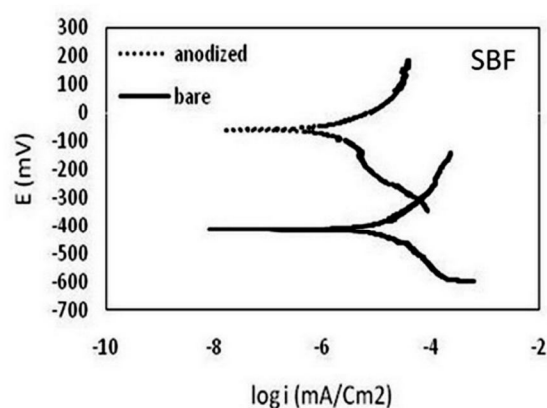


Fig. 5. Potentiodynamic polarization curves for anodized and bare NiTi alloys in SBF and Ringer solutions.

such as electrolyte composition, electrolyte concentration, anodizing duration and etc. By varying these parameters, it is possible to reach the desirable oxide layer thickness which is proportional to working prospects of the sample. However, in the previous studies which have aimed anodizing treatment of NiTi alloys in sulfuric acid electrolyte, obtaining such a large thickness of 13  $\mu\text{m}$  has not been reported. The formation of this thick layer is due to the alteration of different anodizing parameters and finally selecting the appropriate parameters.

The Potentiodynamic polarization curves for anodized and bare NiTi alloys in SBF and Ringer solutions are given in figure 5. Tables 3 and 4 present corrosion parameters of the anodized and bare samples in SBF and Ringer solutions

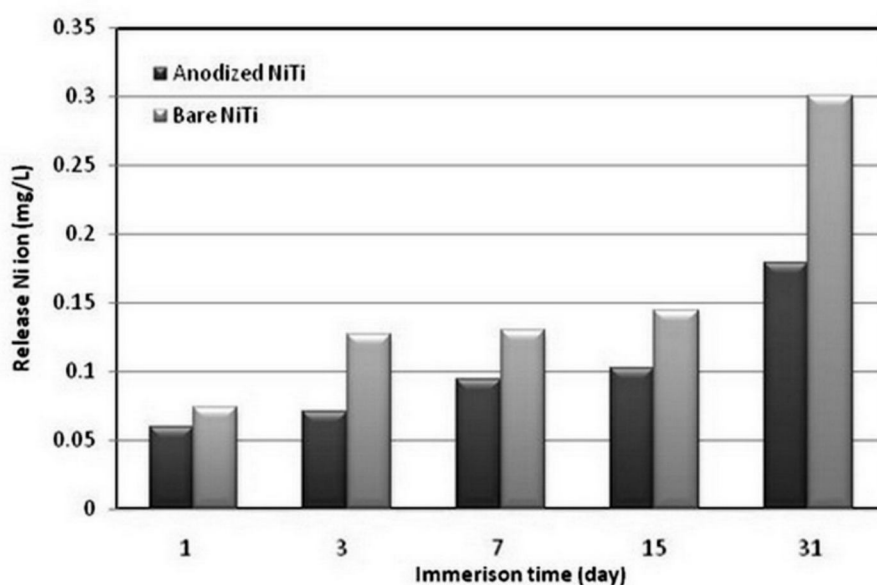
Table 3. Corrosion parameters of the anodized and bare samples in SBF solution.

samples	E <sub>corr</sub> (mV)	I <sub>corr</sub> (mAcm <sup>-1</sup> )	R <sub>p</sub> ( $\Omega\text{cm}^2$ )
Bare NiTi	-400.14	0.002232708	16417
Anodized NiTi	-79.63	3.81285E-05	1.00E+06



**Table 4.** Corrosion parameters of the anodized and bare samples in Ringer solution.

samples	Ecorr (mV)	Icorr (mAcm <sup>-1</sup> )	Rp (Ωcm <sup>2</sup> )
Bare NiTi	-426.78	4.34783E-07	1.00E+06
Anodized NiTi	-187.189	7.24638E-08	6.00E+06

**Fig. 6.** Content of Ni ions, released from the bare and anodized NiTi alloys.

respectively. It can be seen that, in both corrosion mediums, anodizing causes a lower corrosion current and a higher corrosion potential compared with the bare NiTi sample. In other words anodizing significantly improves corrosion resistance. According to Shi et al [19] and Wang et al. [29] studies, the enhanced corrosion behavior is attributed to the formation of an oxide layer on the surface which protects the substrate against corrosion. Thus, it can be mentioned that a thicker oxide film could be more preserving and preferable.

Figure 6 illustrates the cumulative concentrations (mg. L<sup>-1</sup>) of Ni ions, released in SBF for different submersion periods. It is clearly observed that for all submersion times, anodizing process mitigates the content of Ni ions, released

from the NiTi alloys.

Also, as shown in figure 7, the rate of released Ni ions from both anodized and bare NiTi samples reduces with the increase in the immersion time, but with a larger slope for anodized samples. However the maximum level of released Ni ions, which has been measured on the first day of immersion is remarkably lower than the estimated dietary intake. This is a promising result for long-term applications of NiTi shape memory implants and reduces the concern about their relatively large Ni content and the possibility of triggering allergic and toxic reactions in the surrounding tissues [29].

Figure 9 reveals SEM micrographs of the anodized and bare NiTi alloys which have been immersed in SBF solution for 30 days. As can be

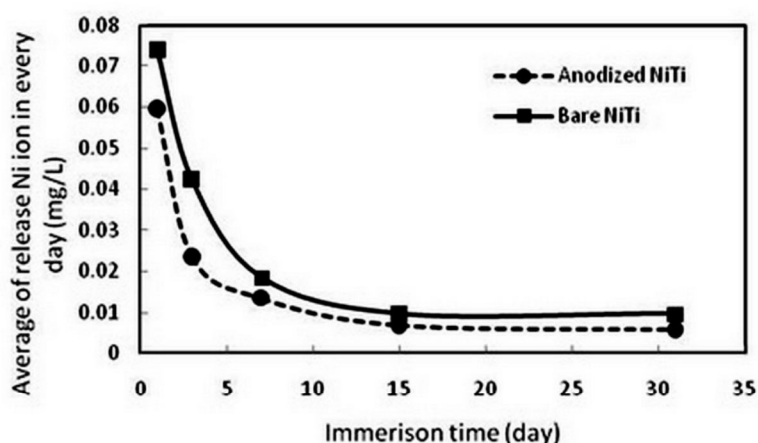


Fig. 7. Rate of released Ni ions from anodized and bare NiTi samples into SBF solution.

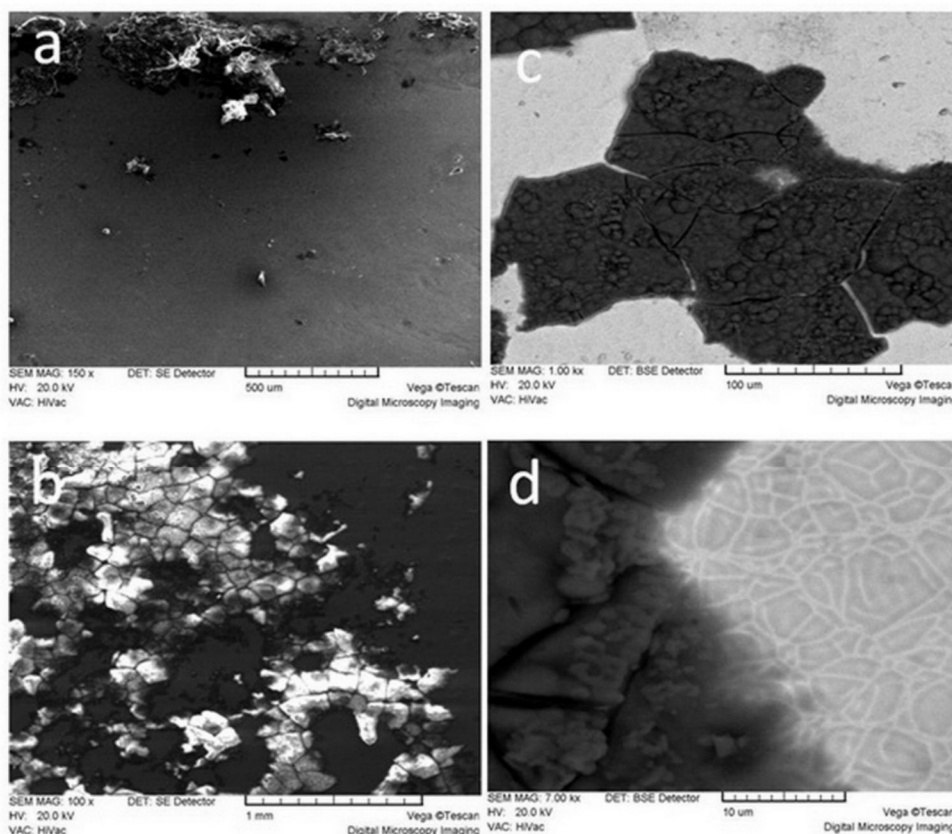


Fig. 8. SEM micrographs of the anodized and bare NiTi alloys immersed in SBF solution for 30 days; a) Secondary electron SEM image of bare sample, b) Secondary electron SEM image of anodized sample, c and d) Back scattered electron SEM images of anodized sample with higher magnifications

seen, the amount of deposited hydroxyl apatite (HA) on the anodized sample is much more considerable compared with the bare sample.

This is ascribed to the  $\text{TiO}_2$  oxide layer, formed on the surface of alloy [30].

Further increase in thickness and porosity of

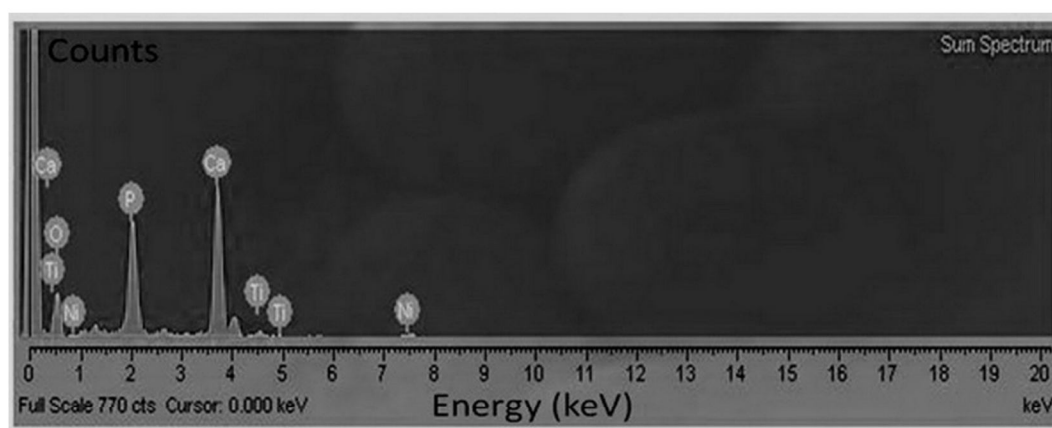


Fig. 9. EDS-spectrum of the deposits on anodized NiTi.

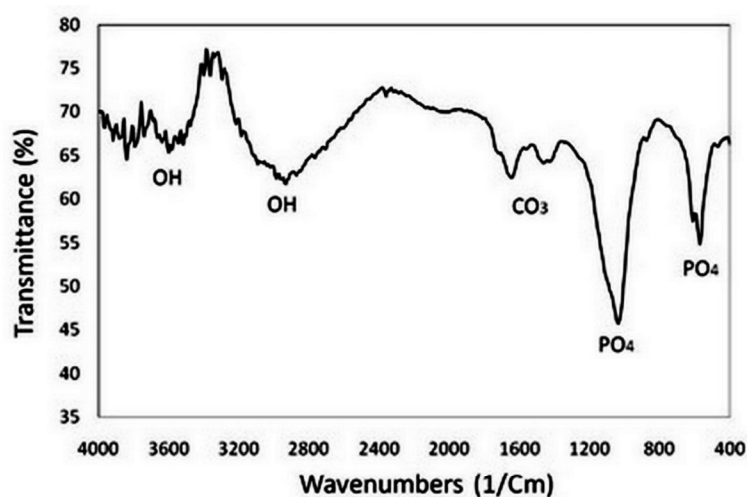


Fig. 10. FT-IR spectrum of the deposits, formed on the surface of anodized NiTi sample.

the oxide layer causes increase in HA deposition. As previously shown, anodizing has raised the surface roughness. Thus, this is another reason for enhanced HA deposition on the surface of anodized alloy. In order to verify the nature of the deposits, EDS and FT-IR analyses were carried out. EDS-spectrum of the deposits is demonstrated in figure 8. Ca, P and O spectra present in this graph may prove that the deposits formed on the surface are HA.

Figure 10 illustrates FT-IR spectrum of the deposits. Absorption peaks at 600 and 1050  $\text{cm}^{-1}$  are related to  $\text{PO}_4^{3-}$ . The peak at 1670  $\text{cm}^{-1}$  is ascribed to  $\text{CO}_3^{2-}$  which both are the ions present

in HA. The bands with wave numbers in the range of 3600-4000  $\text{cm}^{-1}$  are assigned to  $\text{H}_2\text{O}$ , absorbed by the system. There also exist some other peaks at this spectrum which all belong to HA spectrum. The results of two mentioned analyses confirm the presence of HA deposits on the anodized NiTi surface [31-38].

#### 4. CONCLUSION

Anodic oxidation of Ti-50.8Ni in a sulfuric acid electrolyte resulted in the formation of an oxide surface layer with a thickness of about 13  $\mu\text{m}$ . This layer improves corrosion resistance and



Ni ion-release resistance by impeding the direct contact of the alloy with the corrosion mediums i.e. Ringer and SBF solutions. Also the enhancement of biocompatibility of the anodized alloy compared to bare alloy was so satisfying which was related to the roughening of the alloy surface due to anodization. These results show that the NiTi shape memory alloys can be used for long-term applications in the body environment.

## REFERENCES

- Petrini, L. and Migliavacca, F., "Biomedical Applications of Shape Memory Alloys". *Journal of Metallurgy*, 2011. 4: p. 5.
- Duerig, T., Pelton, A. and Stöckel, D., "An overview of nitinol medical applications". *Materials Science and Engineering: A*, 1999. 273: p. 149-160.
- Duerig, T., D. Stoeckel, and D. Johnson. SMA: smart materials for medical applications. *Proceedings of SPIE* 2003, 4763.p 7-15
- Morgan, N., "Medical shape memory alloy applications—the market and its products". *Materials Science and Engineering: A*, 2004. 378(1): p. 16-23.
- Poncet, P. P., "Nitinol medical device design considerations". *Strain*, 2000. 2(4): p. 6.
- Stoeckel, D., Melzer, A. and Vincenzini, P., "The use of NiTi Alloys for Surgical Instruments. *Materials in Clinical Applications*", edited by Vincenzini, P., Techna Srl, 1995: p. 791.
- Esenwein, S., "Influence of nickel ion release on leukocyte activation: a study with coated and non-coated NiTi shape memory alloys", *Materials Science and Engineering: A*, 2008. 481: p. 612-615.
- Vojtech, D., "Surface treatment of NiTi shape memory alloy and its influence on corrosion behavior, *Surface and Coatings Technology*, 2010. 204(23): p. 3895-3901.
- Cui, Z., Man, H., and Yang, X., "The corrosion and nickel release behavior of laser surface-melted NiTi shape memory alloy in Hanks' solution", *Surface and Coatings Technology*, 2005. 192(2): p. 347-353.
- Fernandez, J., "Wear and corrosion of metal-matrix (stainless steel or NiTi)-TiC coatings", *Physics Procedia*, 2010. 10: p. 77-80.
- Pohl, M., "Formation of titanium oxide coatings on NiTi shape memory alloys by selective oxidation". *Materials Science and Engineering: A*, 2008. 481: p. 123-126.
- Rossi, S., "Chemical and mechanical treatments to improve the surface properties of shape memory NiTi wires. *Surface and Coatings Technology*", 2008. 202(10): p. 2214-2222.
- Shabalovskaya, S., Anderegg, J. and Van Humbeeck, J., "Critical overview of Nitinol surfaces and their modifications for medical applications", *Acta biomaterialia*, 2008. 4(3): p. 447-467.
- Shevchenko, N., Pham, M. T. and Maitz, M., "Studies of surface modified NiTi alloy", *Applied Surface Science*, 2004. 235(1-2): p. 126-131.
- Starosvetsky, D. and Gotman, I., "TiN coating improves the corrosion behavior of superelastic NiTi surgical alloy". *Surface and Coatings Technology*, 2001. 148(2): p. 268-276.
- Sun, F., "Surface modifications of Nitinol for biomedical applications. *Colloids and Surfaces B: Biointerfaces*", 2008. 67(1): p. 132-139.
- Xu, J., "Formation of Al<sub>2</sub>O<sub>3</sub> coatings on NiTi alloy by micro-arc oxidation method", *Current Applied Physics*, 2009. 9(3): p. 663-666.
- Zhang, S., "Laser surface alloying fabricated porous coating on NiTi shape memory alloy", *Transactions of Nonferrous Metals Society of China*, 2007. 17(2): p. 228-231.
- Shi, P., Cheng, F. and Man, H., "Improvement in corrosion resistance of NiTi by anodization in acetic acid", *Materials letters*, 2007. 61(11-12): p. 2385-2388.
- Cheng, F., Shi, P. and Man, H., "Nature of oxide layer formed on NiTi by anodic oxidation in methanol", *Materials letters*, 2005. 59(12): p. 1516-1520.
- Yang, C., F. Chen, and S. Chen, "Anodization of the dental arch wires". *Materials chemistry and physics*, 2006. 100(2-3): p. 268-274.
- Cheng, F., "Microstructural characterization of oxide film formed on NiTi by anodization in acetic acid". *Journal of alloys and compounds*, 2007. 438(1-2): p. 238-242.
- Chu, C., "Effects of anodic oxidation in H<sub>2</sub>SO<sub>4</sub>

- electrolyte on the biocompatibility of NiTi shape memory alloy". *Materials letters*, 2008. 62(20): p. 3512-3514.
24. Huang, C., "Enhanced surface roughness and corrosion resistance of NiTi alloy by anodization in diluted HF solution". *Smart Materials and Structures*, 2009. 18: p. 024003.
25. Bayat, N., Sanjabi, S. and Barber, Z., "Improvement of corrosion resistance of NiTi sputtered thin films by anodization". *Applied Surface Science*, 2011. 257(20): p. 8493-8499.
26. Khalil-Allafi, J., Amin-Ahmadi, B., and Zare, M., "Biocompatibility and corrosion behavior of the shape memory NiTi alloy in the physiological environments simulated with body fluids for medical applications". *Materials Science and Engineering: C*, 2010. 30(8): p. 1112-1117.
27. Pramanik, S., "Development of high strength hydroxyapatite by solid-state-sintering process. *Ceramics international*", 2007. 33(3): p. 419-426.
28. Liu, K. T., and Duh, J. G., "Grain size effects on the corrosion behavior of Ni50. 5Ti49. 5 and Ni45. 6Ti49. 3Al5. 1 films". *Journal of Electroanalytical Chemistry*, 2008. 618(1-2): p. 45-52.
29. Wong, M., Cheng, F., and Man, H., "Characteristics, apatite-forming ability and corrosion resistance of NiTi surface modified by AC anodization. *Applied Surface Science*", 2007. 253(18): p. 7527-7534.
30. Bernard, S. A., "Bone Cell-materials Interactions and Ni Ion Release of Anodized Equiatomic NiTi Alloy". *Acta biomaterialia*, (2011) 7 1902-1912.
31. Ciobanu, G., Ignat, D., and Luca, C., "Polyurethane-Hydroxyapatite Bionanocomposites: Development and Characterization". 2009 54(68), pp57-60.
32. Hui, P., "Synthesis of Hydroxyapatite Bio-Ceramic Powder by Hydrothermal Method". *Journal of Minerals & Materials Characterization & Engineering*, 2010. 9(8): p. 683-692.
33. Liu, Y., D. Hou, and G. Wang, "A simple wet chemical synthesis and characterization of hydroxyapatite nanorods", *Materials chemistry and physics*, 2004. 86(1): p. 69-73.
34. Prabakaran, K., S. Kannan, and S. Rajeswari, "Development and characterisation of zirconia and hydroxyapatite composites for orthopaedic applications", *Trends Biomater. Artif. Organs*, 2005 18: p. 114-116.
35. Puska, M., "Synthesis and characterization of polyamide of trans-4-hydroxy-L-proline used as porogen filler in acrylic bone cement", *Journal of biomaterials applications*, 2005. 19(4): p. 287-301.
36. Sadat-Shojai, M., "Preparation of hydroxyapatite nanoparticles: comparison between hydrothermal and solvo-treatment processes and colloidal stability of produced nanoparticles in a dilute experimental dental adhesive", *JOURNAL OF THE IRANIAN CHEMICAL SOCIETY(JICS)*, 2009. 6(2): p. 386-392.
37. Saiz, E., M. Goldman, and A. Tomsia, "FTIR analysis of apatite formation on bioactive glass coatings on Ti alloys", *infrared. als. Materials Science Division*, 2007, (510) 486 491.
38. Simitzis, J., "Synthesis and characterization of acrylic bone cements reinforced with hydroxyapatite", *Journal of Optoelectronics and Advanced Materials*, 2010. 12(5): p. 1213.